MECHANICAL ENGINEERING
UNIVERSITY of WASHINGTON

*Capstone Design Project Winter-Spring 2023*

# Heated Pressure Chamber to Manufacture Skinless Nanofoamed Polymers

**Meza Research Group**

*This project aimed to develop a method of creating open cell nanofoamed polymers for use in potential industrial applications such as filtration and catalysis which are not possible with a skin layer.*

## Final Design Report


## Team Name

Auden Gostin[2], audeng@uw.edu

Ella Kernaghan, [2] ekern@uw.edu

Noah Barrong[1], nbarrong@uw.edu

Christopher Toda[1], ctoda@uw.edu

Nicholas Gower[1], nsgower@uw.edu

[1]Department of Mechanical Engineering, [2]Department of Chemical Engineering

## Under guidance of

Lucas Meza[1], Meza Research Group, lmeza@uw.edu

Eli Patten[1], ME Capstone Advisor, epatten@uw.edu

Ben Rutz[2], ChemE Capstone Advisor, rutzb@uw.edu

[1]Department of Mechanical Engineering, [2]Department of Chemical Engineering

# Executive Summary

This project aimed to create a nanocellular polymer with exposed pores on the skin. Through this effort we were able to successfully create a foamed polymer with a significantly reduced skin thickness. Open-Polymer nanofoams have a wide variety of useful properties and their use for cases like nano-scale filtration and catalysis is limited by their inability to be fabricated with an open skin. The approach used in this project to create one was to first saturate polyethylene terephthalate (PET) with $CO_2$ at 5-6 MPa, and then rapidly heat the polymer with $CO_2$-saturated water above the PET's glass transition temperature. This procedure was conducted multiple times using a system connecting a pressure chamber with a pressurized and heated water reservoir. The outcome was 5 foamed samples of PET. Two of these were analyzed using a scanning electron microscope (SEM) and found to have varied characteristics between the two. One of these samples was found to have a much-reduced skin thickness of 1-3 $\mu m$ compared to polymer foams using traditional techniques.

# List of Figures

# List of Tables

# 1 Project Introduction

## 1.1 Need Statement

A way to address the lack of fabrication method for creating open skin nanofoamed polymers so that the process can be scaled to industry and nanofoams can be used in applications where an unfoamed skin layer prevents their utilization.

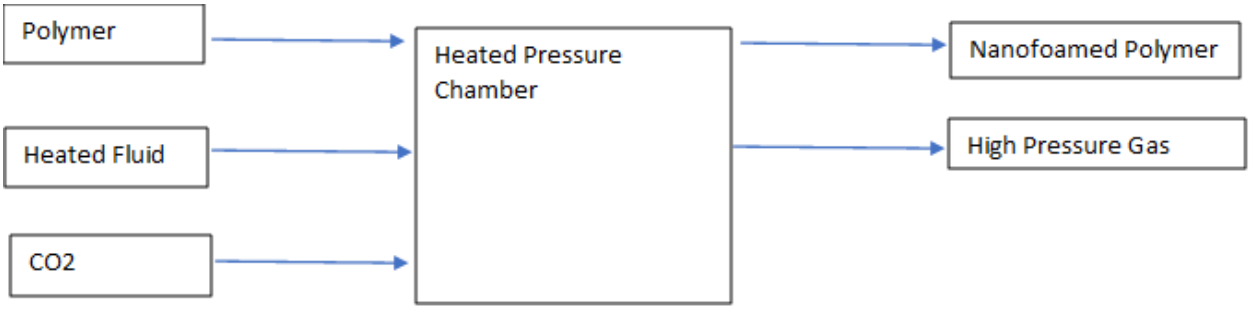


*Figure 1: Single-block function diagram of the Heated Pressure Chamber*

## 1.2 Project Objective

The objective of this project is to create nanofoams without skin. While one of stated goals from Professor Lucas Meza was to scale the process design to industry, as the project progressed, we decided to prioritize the creation of a skinless nanofoam.

## 1.3 Significance and Background

While foams in general have been around for a while, nanofoams are a much more recent area of study. They are interesting for a variety of reasons and provide certain properties that are not available with current materials. Some of these include its low thermal conductivity, low dielectric constant, and high specific strength. Skinless nanofoams have strong potential in the biomedical industry in high performance aerosol filters, which could be used in respirators to combat airborne pathogens. The recent pandemic has shown that such respirators could have ramifications for billions all over the world. Another use that nanofoams bring to the table is their possibility to be used as biological filters for nanoparticles. Also in the biological realm, nanofoams with exposed skin provide a higher surface area for tissue to attach to compared to a solid unfoamed surface. The high surface area also gives nanofoams potential for use in catalysis. With these possibilities in mind, we have been tasked with designing a method of manufacturing this material. If we are successful, nanofoams could one day become a common material in these fields.

Nanofoams are currently produced by gas dissolution foaming which includes three steps: saturating a thin polymer sample with high pressure gas (either CO2 or N2), removing the sample from high pressure, and rapid heating of the sample usually by submerging it in a hot oil bath. The time between depressurizing and heating allows for gas on the surface to escape, creating a concentration gradient of gas in the sample. This causes the outside edges to be unaffected by foaming; they do not form bubbles

and remain an unfoamed “skin” layer. The purpose of this project is to produce nanofoams without a skin layer, with a homogeneous porous structure throughout the entirety of the thickness of the polymer sheet.

## 1.4 Existing Solutions

One way to try to create an open-cell structure is to remove the skin layer after using normal foaming methods. There have been several different attempts to remove the skin after the foaming process, however none have had successful results. For example, polishing the skin layer damages the structure underneath, creating another even denser skin-like layer. Other attempts of drilling to connect the porous structure to the outside of the skin also resulted in damage to the sample. Reactive ion etching and laser ablation were also unsuccessful because the porosity is not very well controlled and that is only reasonable with small samples due to inefficiency. Therefore, a method of producing the nanofoams without a skin to begin with seems to be a better option than trying to remove it from existing skinned-nanofoams.

Other attempts to create skinless nanofoams have focused on using diffusion barriers, with mixed results. One of these studies used a metallic mold as a gas diffusion barrier which achieved a more homogeneous structure, however it restricted the expansion of the plastic during foaming. This meant that it was not possible to significantly lower the density using this method, which is an essential feature of nanofoams that give the more unique properties. In addition, the saturation time was significantly higher due to the gas having to travel through the greatest dimension of the sample instead of being able to travel through the full surface area of the sample. Several other methods have similar issues with being impractical and producing limited improvements upon classic gas dissolution foaming. One notable advancement is the use of a poly-vinyl-alcohol (PVOH) layer for a barrier to gas diffusion which allows for expansion of the foams and prevents gas diffusion out of the edges of the sample during foaming. The layer of PVOH was removed by simply stirring the sample in water and the samples showed a decrease in unfoamed skin layer thickness from 80 μm in the uncoated control to 10-15 μm with the PVOH coating. Additionally, the PVOH coating induces pore formation on the order of the reduced skin thickness which allows for the external skin surface to be partially foamed although not homogeneous with the inside. This project aims at improving upon those results by completely eliminating the skin and using a method that does not require the extra steps and materials of thermoforming the diffusive barrier and then removing it.

In addition to the initial literature review findings on the mechanisms and conditions for foaming as well as the materials’ properties, more information has been gathered on different attempts at scaling the process to industry. For example, Aher, B. et al used commercially available sheets of polyetherimide (PEI) in a scaled-up version of the classic gas dissolution method where sheets were pressurized, allowed to desorb, and then heated between hot press plates lined with fiberglass fabric to allow expansion and gas release during foaming. They found significant blistering occurred with less than 35 minutes of desorption time, and significant curvature of samples when foamed in less than 3 minutes (Aher, Kumar, and Olson 2013). These are both well beyond our expected time frames, with the goal of no desorption and near instantaneous foaming, so we may need to consider these effects later on as we learn how foaming under pressure affects necessary parameters. Another study using polymethyl methacrylate (PMMA) found that sandwiching the sample with polytetrafluoroethylene (PTFE) and glass fiber

composite could prevent blistering in contact heating with a hot press. The rough surface finish of the glass-fiber composite allowed gas to escape from the interface with the hot plate, though it adversely affected the surface finish of the sample as well.

Research into existing solutions gave insight into what variations of gas dissolution are not successful in producing skinless nanofoams and what problems may arise, such as blistering. However, none of the existing solutions attempted eliminating desorption time by heating at saturation pressure. Thus, heating under pressure remains an unexplored option for gas dissolution foaming to potentially create skinless nanofoams.

### 1.5 Stakeholders

As the sponsor of our project, the Meza Research Group is a primary stakeholder. The Microcellular Plastics Lab at UW would also benefit as they stated that the skinless nanofoam problem we are working on was something they had also planned on tackling in the future. The Meza Research Group is providing funding through a budget granted by the National Science Foundation. The Microcellular Plastics Lab is making available certain equipment for requisition, including a cart of old experiment supplies. The findings of our project would likely be available for both groups, likely furthering their research and by proxy, reaching the wider academic community through whatever future related papers they publish. While both industry and research have interest in the development of manufacturing techniques for skinless nanofoams, industry places a greater emphasis on the economics which will make it important for factors such as cost and production time to be placed under consideration to allow the final process to be scaled up in the future.

## 2 Problem Statement

### 2.1 Needs Research

The potential applications of a novel process for the production of nanofoam materials include usage in improving air filters, PPI equipment such as gas masks and disposable face masks, and chemical separations. A nanofoam with an engineered pore size could be specifically designed to provide as a filter for specific chemical separation problems that require a specific pore size. Such a material would have the potential to reduce industrial energy usage as chemical separations are a significant source of industrial energy use.

### 2.2 Customer Requirements

The main requirement is that there is no skin layer on either side of the PEI sample. This is what makes the material unique and gives the ability for its use in various new applications.

A few metrics that are also pertinent to the effectiveness of our product are the density, void fraction, pore sizes, and skin thickness. Pore size is especially critical because by definition, a nanofoam has pores that are on the nano-scale. As such, we must aim for the pore sizes to be in this range. Skin thickness is also a critical quantity. The goal of the project is to have a skin thickness of zero, however, if some samples are produced with a skin, it will be useful to be able to measure this quantity. An interesting property of certain nanofoams is that they can have lower thermal conductivity than air, due to the

Knudsen effect. To achieve this, our samples' densities will need to be around 0.1-0.2 g/cm$^3$ with a pore size of less than 100nm. This density range is not critical but should be considered when analyzing the results of the experiment. Void fraction also does not have a critical value to meet but will tell us how much open space there is in our product.

## 2.3 Engineering Specifications

The saturation pressure and foaming temperature are the key specifications of the design because they affect the size of cells and nucleation density. PEI was chosen as the polymer material because of access through the Microcellular Plastics Lab and the relatively high glass transition temperature of PEI. This is important because if we are able to form a skinless nanofoam with PEI, it will be simple and achievable to reduce temperature requirements in the future for a wide variety of other polymers.

### 2.3.1 Pressure Requirements

To reach nanoscale pores in a PEI sample, a pressure of at least 5 MPa is required. Below this, larger pores form which is undesirable because microfoams do not display the same properties as nanofoams. The amount of time it will take to saturate both the sample and water with $CO_2$ is another consideration when implementing the design. While using 5 MPa for sample saturation (on the lower end of the possible pressure range for nanofoam A pressure of at least 5 MPa is required to reach nanoscale pores in a PEI sample) makes the design safer and loosens requirements on pressure ratings, the downside is that saturation time is longer and concentration of $CO_2$ is lower than at higher saturation pressures (Figure 2). It would be beneficial to consider saturating the sample at higher pressures in future design iterations by adding a compressor. Ensuring that the materials in the final design are safely used for a range of pressures higher than anticipated will work in our favor by having the flexibility of adjusting as needed, either for better properties of foams or for time efficiency. In an industrial setting, operating at a higher pressure would also be preferrable to produce the nanofoams at a higher rate, although there will be constraints depending on the necessary concentration at saturation to reach the desired properties of the foam. The saturation concentration of $CO_2$ in PEI follows Henry's law with a constant of approximately 18.55 mg $CO_2$/g PEI/MPa at 21$^o$C.

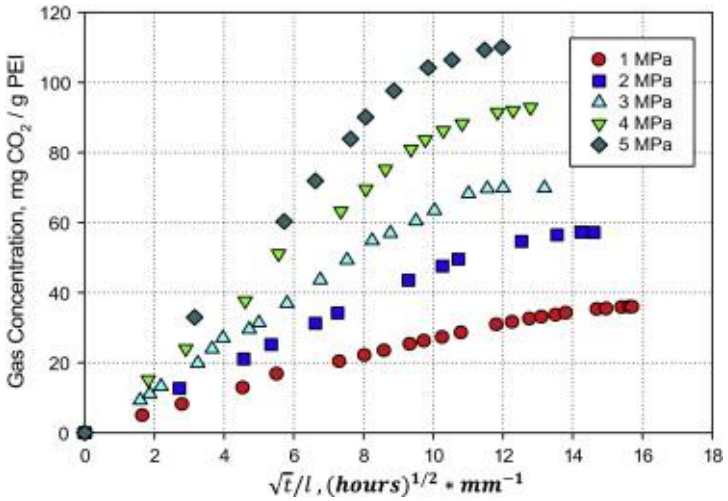


*Figure 2: Gas concentration over time for PEI samples normalized by thickness [1]*

We will be able to run tests on several thicknesses of PEI samples: 0.025 mm, 0.050 mm, 0.12 mm and 0.5 mm. For a 0.025 mm sample at 5 MPa, saturation time will be about 10 minutes, for 0.12 mm sample at 5 MPa, saturation time will be approximately 2 hours, and for a 0.5 mm sample at 5 MPa, saturation time will be approximately 36 hours (Figure 2). Thickness is a consideration because of the impracticality of spending two days waiting for the sample to saturate, limiting the number of samples we would be able to produce over the duration of the project. For the sake of efficiency, it will be beneficial to work with thinner samples initially. Observing potential differences between products of varying thicknesses could also be interesting in directing future research on tuning the properties of nanofoams produced by our new method.

**2.3.2 Temperature Requirements**

The saturation temperature of the sample chamber will be room temperature (21 C), and the saturation temperature of the water reservoir will be the set foaming temperature. The necessary foaming temperature depends on the glass transition temperature of the polymer because of the mechanism of nucleation and cell formation during foaming. The glass transition temperature varies depending on the concentration of CO2 dissolved in PEI at saturation, which is directly proportional to the chosen saturation pressure (Figure 2). A possible foaming temperature range of 80-170 C was found from literature for a PEI saturation pressure of 5 MPa. Within this range, the density of the final product also depends on the foaming temperature, with density decreasing as temperature increases.

We will be first operating at 150 C because according to literature, this should be adequate for a PEI sample saturated at 5 MPa. It should be noted that these temperatures were recorded in literature for foaming done at atmospheric pressure, after depressurization. Because we are eliminating this step and foaming at much higher pressure than atmospheric, it is possible that the temperature required may actually increase to overcome the energy barrier to nucleation. We cannot be sure of this effect or estimate how much the necessary foaming temperature would change since it has not been researched before. The effects of foaming under pressure will be observed when analyzing the foamed samples. This is another reason we have chosen to make a design compatible with a range of pressures and

temperatures rather than specific set points; we may need to adjust conditions depending on the effects of high pressure on the thermodynamics of foaming.

## 2.4 Codes and Standards

Designing a heated pressure chamber requires by law adhering to the ASME Boiler and Pressure Vessel codes, particularly codes related to power boilers and pressure vessels. Initially, this was a concern to us because we anticipated the need to design and manufacture a pressure vessel of our own design. However, since our final design no longer incorporates a custom-designed pressure vessel, we do not have to worry about these codes.

## 2.5 Assumptions

At the temperatures and pressures our pressure chamber will be operating, it is not reasonable to assume that gases act ideally, so we assume Van der Waals equations are accurate for modeling $CO_2$. We also assume that the saturation of water will take less time than the saturation of the PEI sample based upon literature reviews of each, therefore saturation time will be determined by the PEI sample thickness only.

## 2.6 Design trade-offs and challenges

One of the greatest challenges of this project is deciding on the correct balance of gas dissolution pressure and temperature of heating. The saturation pressure, saturation time, heating time, as well initial and final temperatures are all parameters that can be manipulated during testing to get different results. Currently conducted research has given contradictory claims on what pressure and temperature values are most effective at producing nanofoamed polymers. Additionally, as discussed previously, previous findings may not be applicable to foaming under high pressure. Therefore, the design will be flexible to make adjustments to temperature and pressure to achieve the desired results.

# 3 Conceptual Design, Evaluation, and Selection

## 3.1 Project Decomposition

The production cycle of our polymer can be broken down into seven steps, six of which occur within the pressure chamber, and one of which will occur in a separate heating system because rapid heating is required. From these steps, we get six subsystems: Pressure chamber, CO2 intake, heat intake, depressurization system, over pressurization protection, and heat accumulator, shown below in Figure 3.

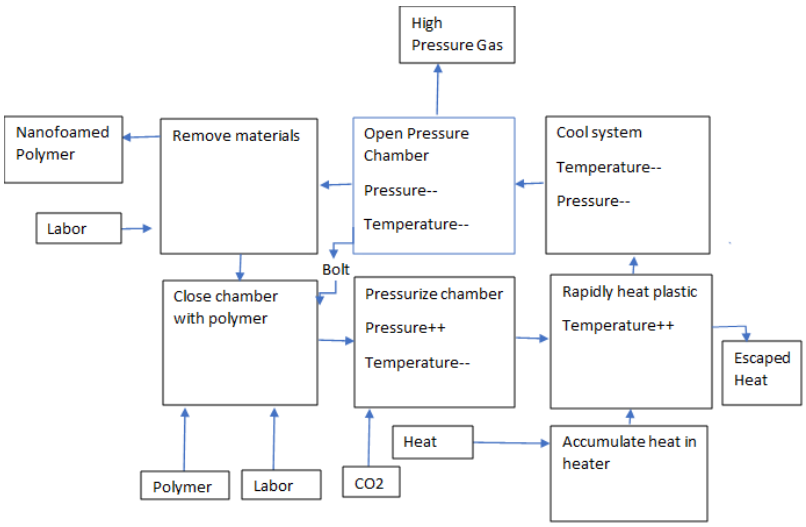


*Figure 3: Project decomposition block diagram*

## 3.2 Concept Generation

After splitting the project into a pressure chamber and heater, we generated several heating concepts. First, we considered four heating methods to potentially incorporate into the pressure chamber: conduction, convection, radiation, and induction. Radiation was ruled out on the basis that bulbs could not withstand the high pressure inside the chamber. Induction was also eliminated because it would not be feasibly rapid enough heating for foaming to occur. Conceptual designs for conduction and convection were made as the remaining options.

## 3.3 Conceptual Designs

The design for conduction utilized rollers on the inside of the chamber which would be heated to the foaming temperature. The main idea was that as the saturated PEI sample was pulled through, it would be heated to the desired temperature, and the whole process being under high pressure would prevent desorption from occurring at the surface of the sample, therefore eliminating the skin layer.

We also researched and designed a method of convection for comparison. This entailed a secondary fluid reservoir heated to foaming temperature from which fluid would flow into the sample chamber. Because this method was also to be done at saturation pressure, desorption would be prevented as the same logic applies that did for the conduction method. In addition, the CO2 concentration gradient would be reduced by utilizing the solubility of CO2 in the fluid.

To compare the two general ideas, we created a table to organize thoughts on the benefits and drawbacks of each design (Table 1). After thoroughly considering the conduction option, it was found to present four main issues: chamber size, blistering, contact pressure, and surface finish. Because having the rollers inside the chamber is required to complete the foaming process at saturation pressure, several electrical components would also need to be inside the chamber, including a motor. This increases the minimum size of pressure chamber, which raises the cost and materials required. Blistering is when the internal porous structure of the nanofoam is destroyed and has been found to occur with the use of hot plates. Contact pressure of hot plates also causes damage to the porous

structure and affects the surface finish of the sample. With hot rollers having a similar heating mechanism, there was concern that our samples' structure would be ruined by blistering and contact pressure using this conduction method.

The convection design poses its own challenges as well including more safety concerns to be evaluated and each additional fluid pipe being an additional failure point. The greatest advantage to using a fluid for heat transfer is that it is already the current method most widely used in the form of a hot oil bath. Therefore, we already know that blistering and other damage to the sample is not a concern with fluids.

*Table 1: Comparison of Pros and Cons of Heat Transfer to the Polymer by Conduction and Convection*

| | **Benefits** | **Drawbacks** |
|---|---|---|
| **Conduction** | 1. Smaller number of pipes reduces risk of pressure-related failure<br>2. Theoretically easier to scale up | 1. Blistering of the sample<br>2. Blistering can be mitigated by use of sandwiching layers, but this adversely affects the surface finish and complicates production.<br>3. Contact pressure adversely affects internal structure.<br>3. Larger pressure chamber required to fit electronics and internal devices<br>4. Concerns with heating of motor and other electrical components |
| **Convection** | 1. Compatible with any size of pressure chamber<br>2. Easily tunable to different conditions<br>3. Can produce multiple samples at once<br>4. Feasible for scaling to industry<br>5. Submersing in an oil bath is already commonly used for foaming | 1. Safety concerns with heated and pressurized fluid<br>2. Need heater<br>3. Has more piping than the convection method which provides more possible failure points |

The convection method was chosen over the roller conduction heating method. While both methods were theoretically capable of meeting the critical customer requirements of heating a polymer under pressure to create a nanofoam polymer without a skin, in concept evaluation, the convection method was found to be much more practical than the conduction method. Research using conduction heating had encountered blistering and offered no satisfactory solution to mitigate the issue. Blisters in a sample would collapse surrounding nanofoam structures, and possibly create a new skin layer defeating the purpose of the process. The only solution offered was to place another layer of plastic over the sample during saturation and heating, but we projected that this would increase saturation times beyond a practical period. Our convection method is essentially a variation of a popular nanofoam heating technique which is not known to have such issues.

## 3.4 Feasibility Analysis

### 3.4.1 Fluid choice

Although the heating step of foaming is normally carried out in a hot silicone oil bath, we have decided to use water for our design. The main reason that oil is used over water in current methods that involve depressurization and heating at ambient pressure, is because water could not be in liquid form in many cases where foaming temperatures exceed 100°C at atmospheric pressure. This is not a concern for our design as water is liquid over all ranges of conditions decided upon. Additionally, there are several advantages to using water in our design including that it is much less expensive than silicone oil, very well documented in terms of physical properties, and allows for higher solubility of $CO_2$. The higher the concentration of $CO_2$ in the fluid, the more it will reduce the diffusion rate out of the PEI sample, the more effective at preventing skin formation. According to Figure 2, the solubility of CO2 in PEI is approximately 110 mg CO2 per g PEI. Assuming a density of 1.3 g/cm$^3$, this is equivalent to a CO2 concentration of 0.143 g/cm$^3$ in PEI. The solubility of CO2 at 150 C and 5 MPa is about 0.35 mol/kg of water [2]. According to NIST, the density of water at these conditions is 0.919 kg/L, so the concentration of CO2 is 0.0142 g/cm$^3$. Therefore, the concentration of $CO_2$ in PEI is significantly higher than in water. There will still be a concentration gradient from the sample to the water, however it will be reduced compared to heating with unsaturated fluid.

The safety risk of using water compared to oil under high pressures and temperatures was the only initial concern. However, with careful design to ensure the water will not escape until controlled depressurization of the system it was determined that there is manageable risk of using water, even at the foaming conditions of 5 MPa and 150 C.

### 3.4.2 Flow Characteristics

We wanted to know if the flow through the pipes would induce turbulence, as opposed to a smooth laminar flow. This could have been a factor in uniformity of heating and safety. Calculating the Reynolds number of water flowing through the pipes, we found that for 0.25” inner diameter, a flow velocity of 6 cm/s would be required to reach the critical Reynolds number of 2000. Therefore, we are confident that it will be turbulent flow in the system.

Upon further research, we concluded that turbulent flow would not have an impact on the results of the experiment. Additionally, after iterations of the design, we have determined that there is no safety risk with superheated water spraying within the chamber.

$$Re = \frac{uD_H}{\nu}$$

$$Re_{cr} = 2000,\ u = \frac{Re_{cr}\,\nu}{D}$$

## 3.5 Concept Evaluation

### 3.5.1 Pressure Driven Flow

One method of flowing water into the sample pressure chamber is to saturate the water at a higher pressure in the reservoir. The main concern for feasibility is the pressure difference between the chamber and reservoir required for adequate flow into the chamber. Initial calculations relied on the conservation of mass and the expansion and compression of $CO_2$ in the water and sample chambers respectively to model the equilibrium condition for water to be fully transferred to the other chamber.

These calculations included several assumptions including that water is incompressible, $CO_2$ can be modeled accurately using Van der Waals equation of state, and all inlets and outlets of the system are closed when the valve between the chambers is opened, and water begins flowing (Figure 4). All volumes of chambers were also assumed as these calculations were done before knowing what materials we had accessible access to including dimensions of the pressure chamber that we ended up using.

The known variables in this case are the saturation pressure of the sample, foaming temperature, room temperature, the initial volume of $CO_2$ in the water and sample chambers, and respectively, the universal gas constant and the Van der Waals constants for CO2. The final volume of $CO_2$ in the sample chamber is calculated by subtracting the volume of water from and accounting for expansion of the sample, and the volume of water is added to get the final volume of $CO_2$ in the water chamber.

The unknown variables are the moles of $CO_2$ in the headspace of the water chamber, the moles of $CO_2$ in the headspace of the sample chamber, saturation pressure of the water, and the equilibrium pressure of the system.

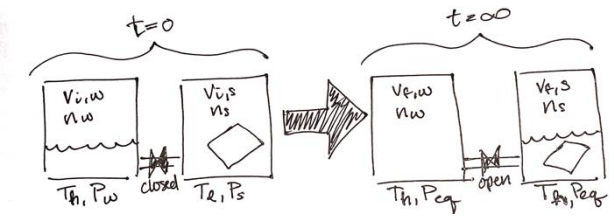


*Figure 4: Visual schematic of the basis for pressure driven flow calculations with conservation of mass*

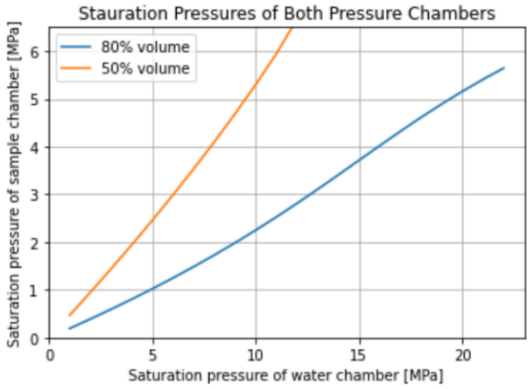


*Figure 5: Saturation pressure of water chamber for varying sample chamber pressures and water volumes*

All volumes of chambers and water were assumed, and these parameters had the greatest impact on the results of the calculations. Figure 5 above shows some of these initial calculations. Therefore, these calculations served as a preliminary means to show what range of pressures or chamber volumes would have to be necessary for this approach to work. Additionally, this method would likely require a second pressure chamber, which in itself, would require approval of designs and machining because of our access to only one pressure chamber. It also would require a compressor to exceed the pressure of the commercially available CO2 tank that our CO2 supply would come from.

### 3.5.2 Gravity Driven Flow

An alternative to pressure driven flow is gravity driven flow. This consists of a reservoir that is elevated compared to the pressure chamber containing the sample, but with equal pressurization on both sides. For feasibility of this idea, the most important factor is the flow rate of the water being fast enough to heat the sample rapidly. With gravity as the driving force, the flow rate of water will be equal at any pressure as long as the entire system is subjected to that same pressure. Therefore, it was easy to determine from a simple test at atmospheric conditions that water will in fact flow fast enough in a variety of configurations. The benefit of this design is that there does not need to be any changes made for tests at different pressures beyond adjusting the regulator. The primary benefit of this design is that we do not need to worry about incomplete flow of the water into the chamber, or backflow.

## 3.6 Concept Selection

Relying on gravity for fluid flow results in a simpler design and for that reason became the focus of the project. However, it was decided that the final design would incorporate the option to also induce a pressure differential between the two reservoirs for flexibility of future testing. This could be useful to run the experiment with a variety of water flow rates, and to attempt to increase the solubility of CO2 in the water without changing the properties of the product by changing the sample saturation pressure. Additionally, the final design has the potential to be attached to a compressor for more flexibility in the range of pressures to test, limited only by the pressure ratings of materials which are well above our current operating conditions. The heater of choice is also able to increase temperature several hundreds of degrees past what we expect. The final concept incorporates gravity and pressure driven flow capabilities, with the ability to easily change pressures and temperature.

# 4 Preliminary Design

## 4.1 Embodied Design

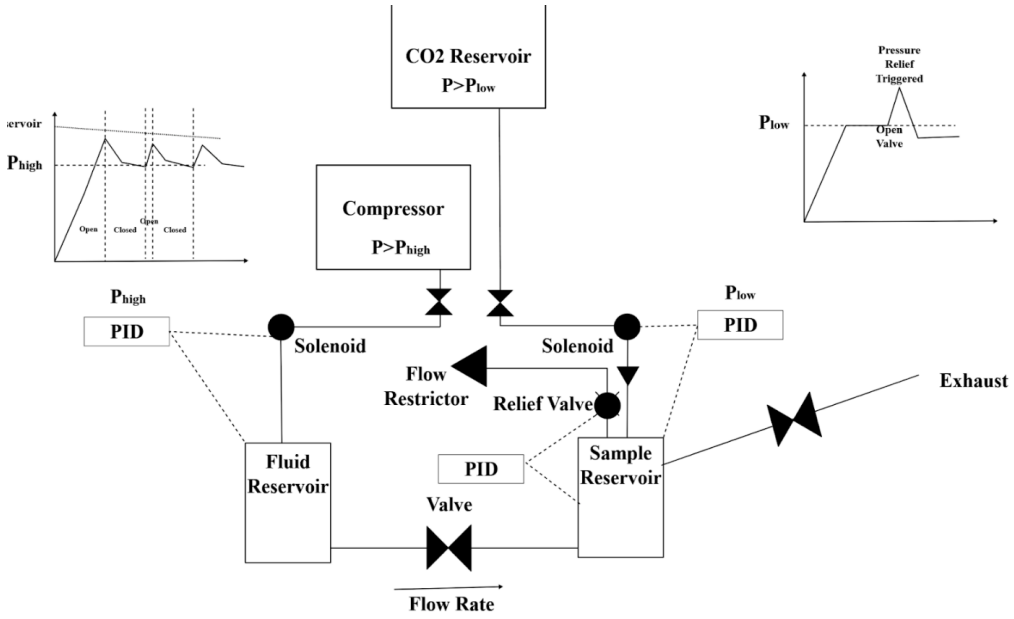


*Figure 6: Preliminary design layout with graphs predicting the behavior of a pressure PID controller.*

The preliminary design was as pictured in Figure 6. The main components of this design included two reservoirs for the sample and water to be separately contained, with two solenoid valves to control the pressure of each side for pressure driven flow, and an unpictured heater around the fluid reservoir. In this design iteration, we planned on incorporating pressure driven flow by using a compressor. This was later determined to be unnecessary as the act of heating the water reservoir would increase pressure enough if closed from the rest of the system. This is further described in the Final Design section, among other design modifications.

The main idea remains the same between this preliminary design and the final design. The water and sample are first separated into their respective reservoirs. The entire system is pressurized, controlled by solenoid valves with PID control systems, and allowed to reach CO2 saturation for both the sample and water. The valve between the reservoirs is opened, allowing the heated water to cover the sample and induce foaming by rapid heat transfer. The release valve is for safety, and the exhaust valve allows controlled depressurization before sample collection. The following sections describe the changes made to this design and the manufacturing process.

## 4.2 Application of Codes and Standards

Designing a heated pressure chamber requires by law adhering to the ASME Boiler and Pressure Vessel codes, particularly codes related to power boilers and pressure vessels. Under these standards, pressure vessels should be designed with a design factor between 4 and 5. Because we decided not to design and manufacture our own pressure chamber, this was no longer a concern. Pipes and all other components

used in the design were rated for pressures greater than the set pressure of our safety release valves, which protects against overpressure scenarios.

## 4.3 Modeling and Analysis

Every component within our design is commercially available, except for the sample chamber which is a pressure chamber provided to us by the Microcellular Plastics Lab. As such, CAD modeling was completed based upon selected parts to decide on a physical layout of the system. The most critical part to model was the fluid reservoir, which is connected to the pressure vessel through a series of NPT pipe connections. This assembly would be the tallest, and heaviest single component in our design other than the CO2 tank. This layout is shown in Figure 7 below.

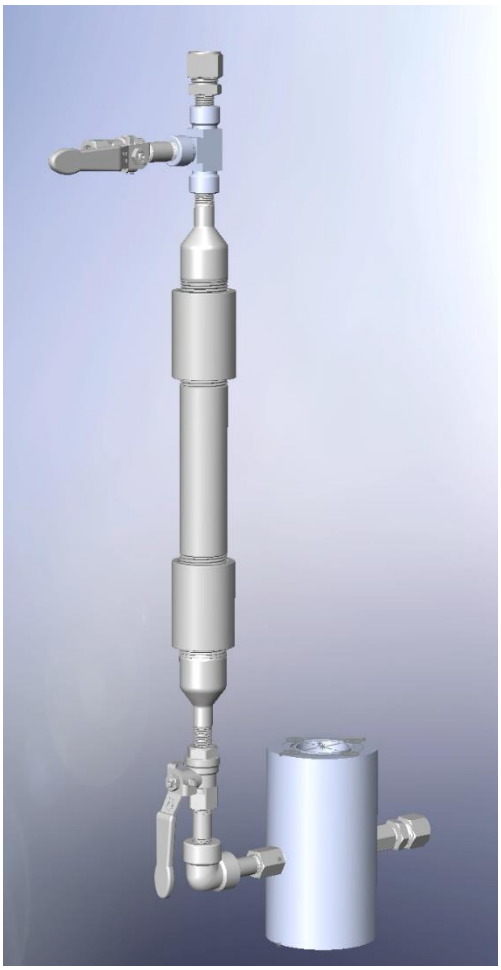

*Figure 7: CAD model of fluid reservoir and sample chamber assembly*

Before we decided against fabricating a pressure vessel, we performed calculations through a Python script to determine the required thickness and bolt quantity for a pressure vessel. This script was later used to determine the pressure rating of our borrowed pressure vessel.

As far as analyzing the product, it is not possible for us to classify properties like pore size, void fraction, or skin thickness using our own tools. These can be found after renting time at an electron scanning

microscope (SEM) to obtain detailed photos of our foamed specimens to determine their properties. The results from this will be discussed later in Section 6.

## 4.4 Prototypes and Testing

During the process of assembling components that we received, we made two major design iterations. Originally, we intended to have two solenoids and two depressurization valves. This was revised to be a single solenoid valve now located in series with the CO2 inlet, and a single depressurization valve, now located near the pressure sensor connected to the chamber. Additionally, a valve was added in series between the tee-pipe that is connected to the solenoid and the tee-pipe that is connected to the fluid reservoir pressure sensor, which will allow a pressure difference to be maintained between the sample chamber and fluid reservoir. We made a preliminary setup of all parts that we anticipated using in our design, with all components that had not arrived yet represented by paper versions. This design is shown below in Figure 8.

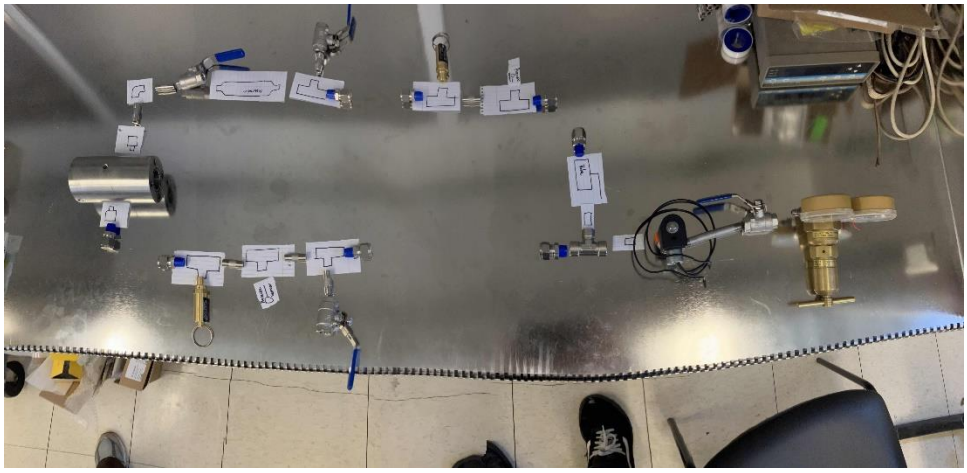

*Figure 8: Partial layout of system design*

# 5 Detailed Design

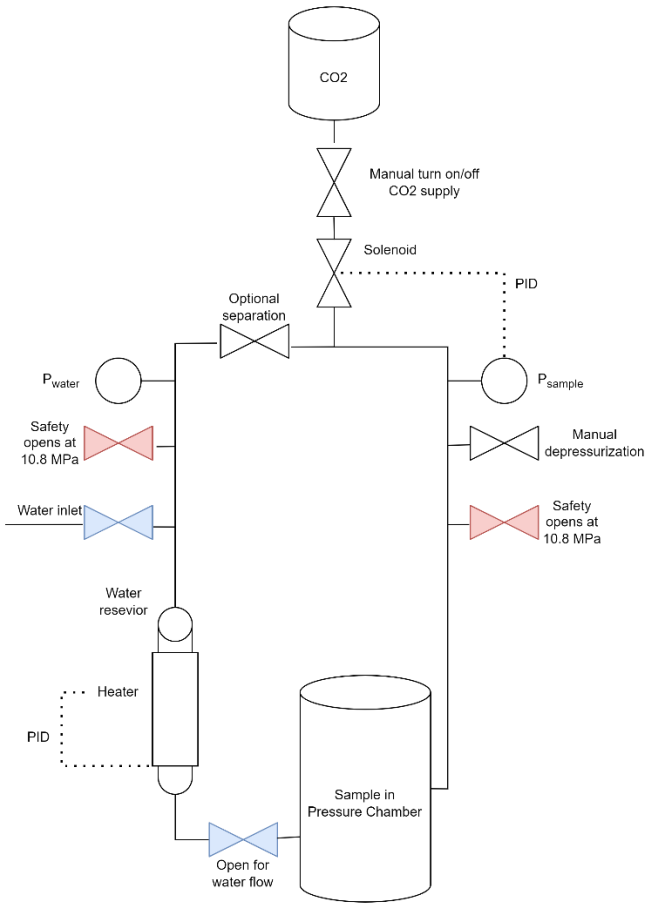


*Figure 9: Final detailed design*

The final design is as pictured in Figure 9. First, the sample is placed in the chamber, and the water is poured into the reservoir using the water inlet valve, ensuring that the water flow valve beneath the reservoir is closed prior. The chamber is then secured, the depressurization and water inlet valves are closed to close the system, and the manual CO2 supply valve is opened to begin pressurization. The system is left for the necessary saturation time to reach the maximum CO2 dissolution with the solenoid valve controlling the CO2 pressure in the system through a proportional-derivative-integral (PID) control system.

The optional separation valve remains open for the entire process unless pressure driven flow is desired in the future, in which case it would be closed at this point. Next, the heater attached to the water reservoir is turned on and the second PID control system maintains the foaming temperature. After sufficient time for the water to reach this temperature, the CO2 supply is closed off and the water flow valve is opened, allowing the heated water to cover the PEI sample, resulting in a rapid heat transfer that produces a nanofoamed sample. About 1 minute later, the manual depressurization valve is opened to control the release of pressure from the system, after which the chamber is opened, and the sample is retrieved for analysis. In addition to those essential components, two safety valves are incorporated

to release pressure if it exceeds 10.8 MPa, which is very unlikely as it is far above the pressure of the CO2 supply and only included as a precaution. This pressure is also well below the pressure ratings of any of the selected components which reduces risk in the case of over pressurization.

## 5.1 Final Design

*Figure 10: Photograph of final assembly.*

An aluminum frame and particle board on top of a cart form the foundation of our system. Four sections of pipes connected by 1/4” tubing are connected to this frame primarily by zip ties. A PID controller circuit regulating temperature sits atop the particle board. A carbon dioxide tank equipped with a pressure regulator supplies CO2 to this system. This network of pipes and pressure vessels forms two pressurized chambers, one designed to contain one or more thin polymer sheets, and the other designed to contain and heat a sample of water. The two systems are connected by a pipe and ball valve at a height difference, with the water vessel being higher than the polymer vessel. Two safety valves designed to release gas at 1500 psi prevent the system from bursting.

*Figure 11: Fusion360 model of final design.*

A complete model of the tubing and piping portion of our design can be seen above in Figure 11. This model preserves the orientations of all the components that we ended up using.

All pressure chambers, tubing, and piping in the system are made of stainless steel, which was chosen due to its strength and anti-corrosion properties. This will ensure that the mixture of water and $CO_2$ does not corrode the system's pipes and cause failure during long-term usage.

Table 2 below is a bill of materials for every part used in the final design.

*Table 2: Final Bill of Materials*

| Component | Specifications | Quantity | Unit Price | Mcmaster part number | Link | Notes |
|---|---|---|---|---|---|---|
| Insulation | 12' by 10' by .5', rated to 2200F | 1 | $ 21.90 | n/a | Amazon Link | |
| corner brackets and t-nuts/screws | need at least ~12 | 2 | $ 18.99 | n/a | Amazon link | 20 corners, 40 t-nuts and 8mm M5 screws each |
| aluminum t-slotted framing | 2020 (20x20mm), 10 4ft segments | 1 | $ 89.89 | n/a | Amazon Link | 40ft total |

| | | | | | | |
|---|---|---|---|---|---|---|
| MDF | 1/2in, 24x24in | 1 | $ 97.39 | 2726N32 | https://www.mcmaster.com/2726N32/ | |
| Braces | 6in long | 4 | $ 17.98 | 5537T2 | https://www.mcmaster.com/5537T2/ | |
| Longer m5 screws | for securing to MDF, 18mm | 1 | $ 10.60 | 91292A127 | link | pack of 50 |
| Chamber bolts | 7/16-14 | 1 | $ 7.81 | 91251A673 | https://www.mcmaster.com/91251A673/ | pack of 10 |
| PID Controller | Voltage: 24 V DC | 1 | 38.58 | n/a | https://www.amazon.com/gp/product/B07XNQ538P/ref=ppx_yo_dt_b_asin_title_o00_s00?ie=UTF8&th=1 | |
| **1 ½" Lg. Male-Male Pipe** | Size: NPT ¼ Thickness Standard: Schedule 80 Expected Parameters: 10 MPa @302° F | 9 | $ 8.40 | 46755K22 | Thick-Wall Stainless Steel Threaded Pipe Nipples and Pipe | |
| **T Pipe** | Size: NPT ¼ Transport gas: CO2 Maximum Pressure: 49.6 MPa Expected Temperature: 72° F | 7 | $ 55.47 | n/a | Stainless Steel Pipe Fitting, Tee, 1/4 in【6,4 mm】, Female NPT | |
| **Manual Valve** | Size: NPT ¼ Temperature: -29°C to 180°C Max Pressure: 2000 PSI | 5 | $ 26.11 | n/a | 1/4" 2000 PSI Ball Valve | |
| **Pressure Transmitter** | Pressure Range: 0-1500 psi, Input Voltage: 9-36 V Interface: NPT ¼ | 2 | $177.05 | | https://www.mcmaster.com/products/pressure-sensors/pipe-size~1-4/maximum-temperature~range~~-1771539818277/maximum-pressure~1500-psi/ | |
| **Pressure Relief Valve(Pop Safety)** | Temperature Range: -20 to 300 F Set Pressure: 1500 psi Pipe Size: NPT 1/4 | 2 | $154.58 | 5825T21 | https://www.mcmaster.com/products/pressure-relief-valves/valve-type~pop-safety/inlet-pipe-size~1-4/set-pressure~1500-psi/ | |
| Ultra-High Temperature Heaters for Pipes and Tubes | Power: 468 W, Lg: 6 ft | 1 | $74.55 | | https://www.mcmaster.com/products/heating-coils/ultra-high-temperature-heaters-for-pipes-and-tubes-7/ | |
| Digi-sense PID temperature controller | | 1 | 0 | | https://www.coleparmer.com/i/digi-sense-standard-temperature-controller-110v/8900000 | already had |
| Type T Thermocouple | Type T, Flat plug | 1 | $30.44 | | https://www.mcmaster.com/products/thermocouples/bendable-thermocouple-probes-for-liquids-and-gases/ | |
| **1/4-1in pipe** | Schedule 80 Stainless steel(Max size=1") | 2 | $ 62.66 | 2161K32 | https://www.mcmaster.com/2161K32/ | |

| | | | | | | |
|---|---|---|---|---|---|---|
| **1in pipe** | 6in long, psi and T spec not given | 1 | $ 47.97 | 46755K76 | https://www.mcmaster.com/46755K76/ | |
| **1in-1in connecter** | 2800psi @350F | 2 | $ 51.65 | 4443K666 | https://www.mcmaster.com/4443K666/ | |
| **1/4in elbow** | 1900psi @350F | 1 | $ 19.24 | 45525K512 | https://www.mcmaster.com/45525K512/ | |
| **1/8in to 1/4in adaptor** | goes into chamber walls, 6000psi @300F | 2 | $ 26.46 | 51205K187 | https://www.mcmaster.com/51205K187/ | |
| **1/4in tubing** | stainless, 6ft lengths | 2 | $ 48.27 | 89895K722 | 89895K722 | |
| **1/4 NPT-1/4 tube adapter** | need at least 10 | 10 | $ 13.05 | 5182K111 | https://www.mcmaster.com/5182K111/ | |
| Grey PTFE Tape | Designed for use with Stainless steel | 2 | $14 | | https://www.amazon.com/dp/B008HPW1HU?psc=1&ref=ppx_yo2ov_dt_b_product_details | |
| TKDY 24V LED Strip Lights Power Supply | Output voltage: 24 VDC<br>Max Power: 36 W | 1 | 11.88 | | https://www.amazon.com/dp/B08MQ2KM2N?ref=ppx_yo2ov_dt_b_product_details&th=1 | |
| Polyimide Tape | 280C rated (2" x 36 yds) | 1 | 12.98 | n/a | https://www.amazon.com/dp/B07HB9M3ZP?ref=ppx_yo2ov_dt_b_product_details&th=1 | |
| Flexible reinforced 1/4" tubing | 1/4" tubing on both ends, 36" long | 1 | 0 | | | already owned |
| Flexible tubing | npt 1/4 to npt ¼, about 36" long, coiled | 1 | 0 | | | already owned |
| Pressure Chamber | Has two 1/8 NPT ports | 1 | 0 | | | already owned |
| Subtotal | | | 2367.41 | | | |
| Tax | | | 236.741 | | | |
| Total | | | 2604.15 | | | |

## 5.2 Manufacture and Assembly

This system was designed to minimize the amount of unconventional machining required, particularly in pressurized components. Machining pressurized components in a way not intended by the manufacturer would require approval from a PE specialized in pressure vessels. This system was designed such that no such approval was necessary. The aluminum beams and wooden board were cut to their final dimensions with a band saw. Beams were connected by 90° angle brackets held in place by

Stainless steel NPT pipes were connected with a pipe wrench. Following conventional methods of permanently installing stainless steel pipes, the male threads of each pipe were wrapped in grey PTFE tape, hand tightened as much as possible, and given three additional turns with a pipe wrench. Brass NPT threads in the CO2 tank were connected in a similar manner, but with white PTFE tape.

Each section of pipes is terminated by multiple NPT-tubing couplings, designed to securely connect sections of 1/4" tubing to NPT ¼ pipes. The tubing was bent with a 1/4" tube bender and cut with a tube cutter. After a preliminary cut and bend were made in each piece of tubing, additional bends and cuts

were made to correct errors made in the first cut and bend and bring the tube to an appropriate shape. Tubes were installed in the system by inserting them into the coupling and tightening the couplings as much as possible with two appropriately sized wrenches.

The heating element was wrapped around the water vessel, with the thermocouple laying between the heating element and the vessel. Both the thermocouple and heating element were bonded to the water vessel by high-temperature tape.

## 5.3 Engineering Economics

We have estimated the operating cost of manufacturing a batch of nanofoamed polymer with our system. As we scale up our system to manufacture larger samples, the initial cost of the system will increase, while the majority of operating costs will not increase. We do not have an effective method of calculating the lifetime of our device, so we will not be taking machine life into account.

Given the numerous issues that our system has encountered with valves breaking during operation, we estimate the maintenance cost of the system to be equivalent to replacing one ball valve for every ten samples.

To estimate the cost of heating the sample, we assumed that our 468 W heater is on 50% of the time over the course of heating for one hour, consuming around 0.25 kWh of energy, costing a total of $0.03.

While this estimate of cost by category is a rough estimate of the actual cost of operating this machine, it allows us to see that over the long term, reducing labor costs by automating the heating process. Replacing the water transport valve with a solenoid valve controllable by a microcontroller will eliminate all need for someone to watch the machine during heating.

$$t_{setup} = 1 \text{ hour}$$

$$t_{heat} = 1 \text{ hour}$$

$$c_{heat} = 0.12 \frac{\$}{\text{kW*hour}} \text{ (Cost of electricity in Washington, 2023)}$$

$$C_{heat} = t_{heat} * c_{heat} * 0.5 * 0.468\ kW = \$0.03$$

$$C_{labor} = 15 \frac{\$}{\text{hour}} * 2 * \left(t_{setup} + t_{heat}\right) = \$60$$

$$C_{operating} = \frac{\$26.11}{10 samples} = \$2.61$$

$$C = C_{heat} + C_{labor} + C_{operating} = \$62.64$$

## 5.4 Budget and Costs

This budget description was provided by Professor Meza at the beginning of the project:

“This project will dedicate $4,000 for the construction of a prototype combined heating and pressure vessel. This will cover the costs to purchase raw materials ($500), fabricate a new chamber ($1,500), create and test a heating system ($1,000), incorporate over-pressurization safety components ($500)

and purchase miscellaneous consumables ($500). “The engineering team expects that the cost of construction will be significantly less than the proposed budget, after having made savings on areas such as the second pressure vessel, heater unit, and consumable parts.

Virtually all of the costs estimated by Lucas Meza were overestimates, but his budget neglected to include several crucial components that are in our final design. The total raw material cost added up to $2604, with the raw materials for foaming costing a negligible amount of money, the new water pressure chamber costing $333.73, the heating system costing $115.75, and the over-pressurization valves costing $340. The majority of our system’s costs came from the valves, tubing, and pipes.

# 6 Verification and Validation

## 6.1 Initial Testing of System Integrity

After fully assembling the system, we performed a pressurization test, where we pressurized the system to the vapor pressure of CO2, then depressurized the system. The purpose of this test was to determine if the system could maintain a high pressure without leaks. This test allowed us to see that the system was properly sealed and could effectively contain 6 MPa of pressure.

During assembly, the heating system was tested several times to determine if it could effectively heat the water without significantly overshooting the set temperature. While there was significant temperature overshoot during initial tests, reducing the temperature controller’s derivative time almost eliminated temperature overshoot. To test the heater’s ability to heat water, we depressurized the fluid reservoir and turned on the heater until water started to boil.

Once we were confident that both the pipe network and heating system were ready, we attempted to create a nanofoam out of a 100 $\mu m$ thick sample of PEI. After completing diffusion, we set the temperature controller on the heater to 150 C, for ten minutes, assuming that would be enough time to heat the water to an appropriate temperature. This test failed to produce a nanofoam. The water was not hot enough to foam PEI.

Before beginning the second foaming test, we reinstalled the heater with more tension than in the first test to increase contact surface area between the heater and fluid reservoir. We also moved the thermocouple from being between the heater and reservoir surface to being on the outside of the heater. The heater was much more effective in this configuration, and during the subsequent water boiling test, water within the system started to boil.

During the second foaming test, we placed another 100 $\mu m$ thick PEI sample into the chamber. For this test, we set the temperature controller to 180 C for around one hour after diffusing CO2 into the sample for 150 minutes. During this test, water leaked out of the Water Flow valve before heating began, meaning that by the time we finished the heating step, all of the water was already in the polymer chamber and was not hot enough. We discovered after this test that the PTFE seals within the water flow and water intake valves failed because temperature exceeded the glass transition of PTFE (120 C) which forms the essential seal in the valves. After replacing both valves that failed, the system was able to hold pressure again. At this point, we decided to switch from PEI samples to polyethylene

terephthalate (PET) which has a glass transition temperature of 80 C and can still be saturated with 5 MPa.

### 6.1.1 Ball Valve Failure

One significant hurdle we experienced during the operation of our final design was that our ball valves unexpectedly failed after one or two uses. Upon inspection of the failed valves, it became aware to us that they all contained PTFE (Teflon) as their seal material. Teflon has a lower glass transition temperature than what we were operating the system around which meant the actuation of the ball valves caused the seals to deform, rendering them unable to maintain pressure differences. A solution to this was devised where critical valves had their seals replaced with ones fabricated out of PEI instead. A deformed seal and a PEI replacement are shown in Figure 12 below. PEI seals allowed us to operate the system up to the glass transition temperature of PEI, which was above what we were anticipating needing for foaming PET.

*Figure 12: Deformed PTFE (white) and new PEI seal (yellow)*

## 6.2 Verifying successful foaming

Our first successful nanofoam was made on May 24, from a 500 $\mu m$ piece of PET, shown below in figure 13. It was immediately clear to use that this sample was foamed successfully because of the dramatic change in opacity, shown in Figure 14. The saturation pressure was 6 MPa, the water was completely unsaturated, and the heater's set point temperature of 140 C ensured the water was heated past the glass transition temperature of PET. The PTFE seals were not damaged, which indicates that the water did not exceed 120 C, the glass transition temperature of PTFE, even though the set point temperature of the heater was 140 C. Therefore, in future testing we are taking into account the temperature difference between the heater and the water, and we recommend in future iterations of the design that a thermocouple be used to directly measure the water temperature.

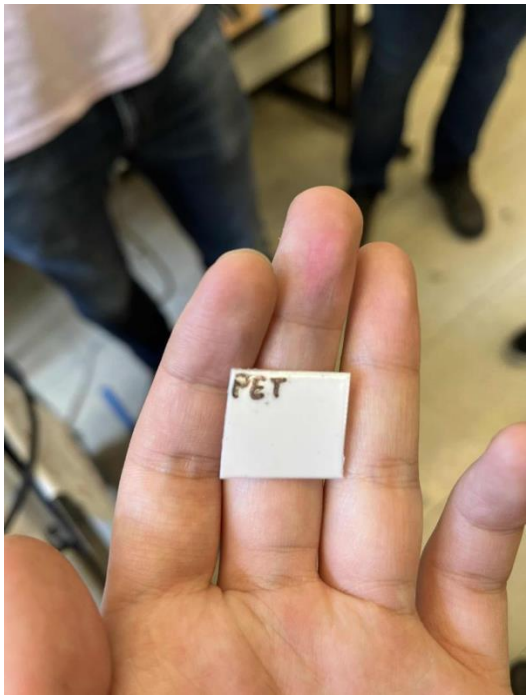


*Figure 13: first successful foamed PET sample*


*Figure 14: Difference in opacity between unfoamed sample (left) and foamed sample (right)*

The SEM images of the first foamed PET sample show a gradient of cell sizes with the core having larger microscale pores and the edges where the skin would be having nanoscale pores (Figure 15). The skin size is approximately 1-3 microns, so with the first foam, the goal has nearly been met of eliminating the skin entirely. However, the irregularity of the cell sizes could be due to two factors which were addressed in subsequent testing. The sample was not fully saturated for sake of time and, meaning the concentration of $CO_2$ in the core of the sample was lower which causes larger bubbles, and the pressure of 6 MPa can cause crystallization to occur in PET which prevents bubble formation. Additionally, the temperature of the water was not high enough to achieve a low relative density foam which is desirable.

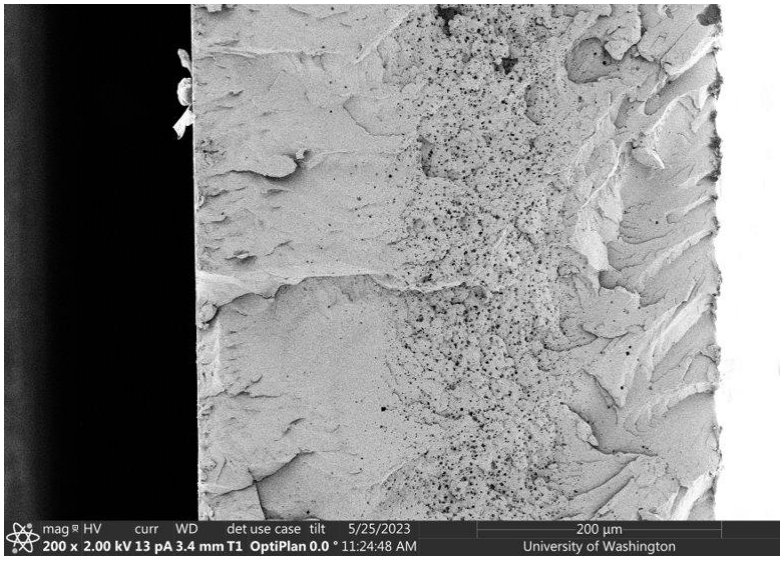


*Figure 15: The first foamed sample*

The second test used saturated tap water at with the same water temperature, and the third test used saturated DI water at 145 C. These were set up before receiving the SEM images from the first test, so the pressure was still at 6 MPa not knowing that crystallization was potentially occurring. The fourth test was set to 5 MPa with foaming temperature of 150 C. To achieve the higher temperatures without damage to the valves, we manufactured seals from PEI to replace the original valve seals made of PTFE. All of the tests have been summarized in Table 3: Summary of experiments and results.

SEM images of sample 4 show a cell size and skin layer consistent with prior literature (Figure 16). There is essentially no difference between this sample and those that result from conventional solid state gas dissolution foaming. This could mean the water was not saturated or that saturating water was not enough to prevent skin formation.

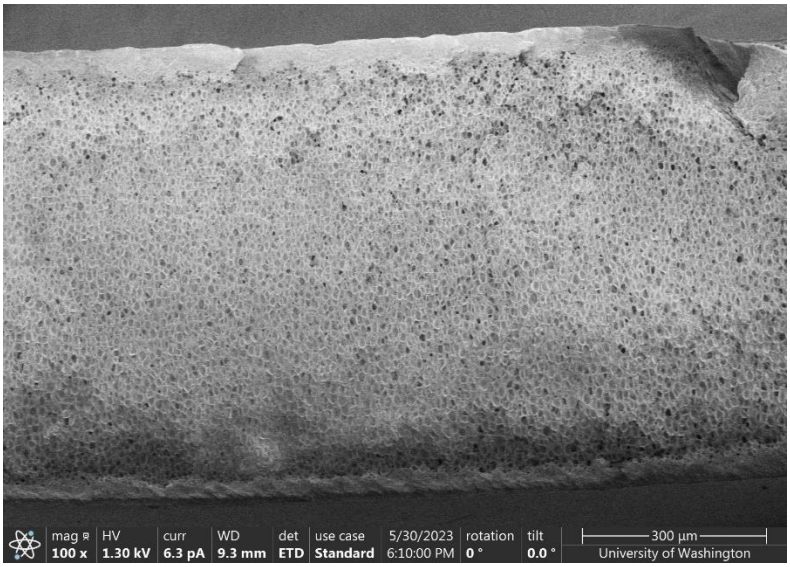


*Figure 16: The 4th foamed sample*

*Table 3: Summary of experiments and results*

| Test number | Saturation Pressure | Water type | Water saturation ? | Heater Set Point Temperature (deg C) | Skin size & Other Observations |
|---|---|---|---|---|---|
| 1 | 6 MPa | Tap | None | 140 | 1-3 µm skin, larger cells in the middle |
| 2 | 6 MPa | Tap | Some | 140 | No SEM image |
| 3 | 6 MPa | DI | Some | 145 | No SEM image |
| 4 | 5 MPa | DI | Some | 150 | 20-40 µm skin |
| 5 | 5 MPa | DI | Some | 165 | No SEM images, less foamed than 4 (less opaque) |

The difference between samples 4 and 5 indicates that 165 was possibly too high of a temperature, as that was the only variable that changed. As the temperature increases, relative density should decrease until a point where the cells start to collapse, therefore it becomes less foamed and less opaque. However, because of our imprecise control over the exact temperature of the water, these set point temperatures do not necessarily

# 7 Discussion

## 7.1 Environment

Plastic already proposes a challenge to protect the environment, with waste exceeding what can be managed. This new type of plastic could increase overall use. However, with recycling methods

advancing and the ability of recycled polymer plastics to be foamed, this should not significantly impact the environment.

## 7.2 Safety and Liability

This project uses pressurized water heated to a temperature beyond its atmospheric boiling point of 100 C. If any pressurized part unexpectedly fails or is otherwise opened while under pressure, this water will instantaneously boil and escape, posing a burn hazard for the user. However, small pressure leaks do not pose any serious risk. To ensure that vessel pressure never exceeds a value that may threaten the integrity of any of the pressurized parts, we have included a pressure relief valve in each sealable pressure section which will vent off excess pressure.

## 7.3 Ethics

While there are potential ethical concerns concerning the safety and environmental impact of our system, those concerns have already been addressed in 7.1 and 7.2. There are no ethical concerns for our project that would not be more accurately labeled as environmental or safety concerns.

## 7.4 Society

Our project, by creating new uses for plastics, may create a demand for plastic that did not previously exist, increasing overall plastic consumption. One possible use for skinless polymers is in reverse osmosis filters. If nano-foamed polymers are found to be emitters of microplastics, and these foams are used to filter water on a large scale, it could expose entire communities to microplastics, causing unknown health effects. We recommend researching the risks of PEI producing microplastics and the potential health effects of such microplastics.

## 7.5 Intellectual Property

Three elements of this project are potentially patentable: The diffusion of CO2 into water before foaming, the use of gravity driven water to heat the polymer, and the use of an external heater around a heated section of pipe. We have filed for a patent through UW CoMotion, and we will learn if we have received a preliminary patent after the submission of this report.

# 8 Conclusion

## 8.1 Summary

This project was partially successful in its endeavor to create a skinless nanofoamed polymer specimen. The final design incorporated a means to foam a polymer while under continuous pressure, which was the primary goal of our design. We were able to successfully operate the system around this goal and created 5 foamed specimens. However, the two foamed specimens that we were able to image and characterize had relatively inconclusive results. These two specimens were not foamed under the same conditions and showed varying skin thickness, pore sizes, porosity, and even opacity. Specimen 1 showed a reduced skin compared to traditionally-foamed polymers, which is promising. However, more testing and characterization of specimens is required before this project can be considered a complete success or not.

## 8.2 Recommendations and Next Steps

As mentioned above, more testing is required to fully determine the effectiveness of our current design. This entails multiple things: running multiple tests under the same conditions to confirm repeatability, testing under more precise conditions to accurately show the polymer's response to foaming parameters, more imaging and characterization of already-foamed samples, and including tests with saturating other kinds of polymers such that the possibility of crystallization is eliminated during saturation. All of these improvements to testing would allow us to have a better idea of how polymers react to the parameters controlled for in our system.

The issue of crystallization was brought up during the very last presentation of this project. Krishna Nadella, who is currently conducting industrial polymer foaming processes in India, mentioned that the cause for a skin in some of our successfully foamed samples may be due to partial crystallization of the polymer chains caused by CO2. Two specific alternatives to saturating PET with CO2 would be to instead saturate PMMA with CO2, or to saturate polystyrene with N2. In these cases, crystallization would not be an issue, which he said he had experienced before.

The system design itself can be improved in four primary ways, those being temperature control, temperature rating, fluid saturation assurance, and repairability.

To have better control over the temperature of the fluid in the fluid reservoir, we would recommend implementing a means of directly measuring the temperature of the fluid inside. One example of how this could be implemented would be to add a thermocouple that screws into the reservoir's pipe assembly using an additional tee-pipe near the bottom of the reservoir.

To increase the system's maximum temperature, we recommend either replacing all PTFE seals in all ball valves with PEI seals or buying valves that do not rely on plastic seals. To increase the system's maximum temperature rating, we recommend either replacing all PTFE seals in all ball valves with PEI seals, or instead using valves that do not rely on plastic seals to hold a pressure. Replacing seals with PEI equivalents would allow our system to instead be operated at temperatures all the way up to the Glass transition temperature of PEI, which is about 180 C. Using valves that do not rely on plastic components would allow the system to be operated up to its initially designed temperature of 250 C, which if PEI foaming is of interest, is necessary.

To ensure fluid saturation, multiple methods could be implemented. One possible way to address this is to use water that is already saturated. This could be done by using store-bought carbonated water, or by using a carbonation system like a SodaStream. Once this CO2-saturated water is inserted into the fluid reservoir, pressurizing the reservoir would ensure that the water does not lose saturation. Another way to address fluid saturation is to use a heating fluid that CO2 has low, or zero solubility into. This would disallow CO2 from the saturated polymer from moving into the heating fluid. One possibility of this kind of fluid that could be investigated further is salt water.

To improve the repairability of valves within the system, replacing sections of pipe between vulnerable components with tubing will make it easier to repair in case of valve failure. Particularly, this would be the pipe section connecting the fluid reservoir to the pressure chamber.

## Acknowledgements

This project stands on the shoulders of dozens of researchers working over the course of several decades. We thank Lucas Meza for organizing this project and for applying for the NSF grant that funded it. Additionally, we thank Vipin Kumar and Santhosh Sridhar of the Microcellular Plastics Lab, and Bill Kuykendall, for consultation and equipment.

# A Bibliography

ASME. (2013). *ASME Boiler and Pressure Vessel Code: An International Code*. Retrieved January 29, 2023, from https://files.asme.org/Catalog/Codes/PrintBook/34011.pdf

B. Notario, A. B.-P. (2016). Nanoporous PMMA: A novel system with different acoustic properties. *Mater. Lett.*, 76-79.

*Cost of electricity in Washington*. (2023, June 5). Retrieved from energysage: https://www.energysage.com/local-data/electricity-cost/wa/

Cuadra-Rodríguez, D. B.-S.-P. (2022). Production of cellular polymers without solid outer skins by gas dissolution foaming: A long-sought step towards new applications. *Materials & Design (Vol. 217)*, 110648.

D. Jose, C. G. (2017). ABRICATION OF BULK SKINLESS POLYETHERIMIDE (PEI) NANOFOAMS. *Proceedings of the ASME 2016 International Mechanical Engineering Congress and Exposition IMECE2016*, 1-8.

D. Miller, P. C. (2009). *Microcellular and nanocellular solid-state polyetherimide (PEI) foams using subcritical carbon dioxide I. Processing and structure*. (Polymer) Retrieved May 12, 2023, from https://www.sciencedirect.com/science/article/pii/S0032386109007770?via%3Dihub

*Fin Convection Experiment.* (n.d.). Retrieved from https://web.archive.org/web/20221025183611/http://courses.washington.edu/me331afe/Fin%20Convection%20Experiment.pdf

H. Yokoyama, T. M. (2000). *Structure of Asymmetric Diblock Copolymers in Thin Films*. Retrieved from https://doi.org/10.1021/ma9912047.

J. Germain, J. F. (2009). Nanoporous Polymers for Hydrogen Storage. *Small.*, 1098-1111.

J. Martín-de León, V. B.-P. (2017). Key Production Parameters to Obtain Transparent Nanocellular PMMA. *Macromol. Mater. Eng., 302*, 3-7.

S. Siripurapu, J. C. (2004). Surface-constrained foaming of polymer thin films with supercritical carbon dioxide. *Macromolecules., 37*, 9872-9879.

S.-K. Yeh, Y.-C. L.-C.-C.-F. (2017). Mechanical Properties of Microcellular and Nanocellular Thermoplastic Polyurethane Nanocomposite Foams Created Using Supercritical Carbon Dioxide. *Industrial & Engineering Chemistry Research*, 8499-8507.

Theodore L. Bergman, A. S. (2011). 7.7: Impinging Jets. In *Introduction to Heat Transfer* (pp. 459-461). John Wiley & Songs, Inc.

V. Kumar, J. W. (1994). A model for the unfoamed skin on microcellular foams. *Polym. Eng. Sci.*, 34.

X. Wang, L. P. (2021). *"Experiment based modeling of CO2 solubility in H2O at 313.15-473.15K and 0.5-200 MPa"*. (Applied Geochemistry) Retrieved May 12, 2023, from https://www.sciencedirect.com/science/article/pii/S0883292721001372?via%3Dihub

# Appendices

# B Project Retrospection

## B.1 Engineering Design Process

The entirety of winter quarter was spent on conceptual design and research. We spent a lot of time trying to figure out what we even were trying to do, as none of us were previously familiar with how solid-state foaming works. As such, much of our time was spent in the ideation and conceptual stage.

At the start of the project, we should have spent more time defining our priorities. We defined our first priority as making an open-celled nanofoam, and we spent a long period of time researching diffusion pressures and foaming temperatures with a premature level of precision. If we spent a shorter period of time finding the maximum temperatures and pressures required, and designed the system to incorporate those values, we would have saved a significant amount of time on design in the early stages of the project.

Our team spent a large amount of time focusing on system elements that could have been useful but were ultimately unnecessary. We found by the end of the project that our system did not require a pressure PID controller to control the system pressure, as an analog pressure regulator controlled the system pressure with a sufficient amount of precision for our purposes.

## B.2 Teamwork and Project Management

Our primary strengths are our teamwork and project management are our task specialization. As a mixed-major group of Chemical Engineering students and Mechanical Engineering students with differing class experience, we all found niches where our experience was helpful.

A couple of weaknesses of our project management were a lack of redundancy in some areas, and a lack of chain-of-command. At the beginning of the project, we only had one team member who was capable of making purchases through PurchasePATH which meant that purchases were sometimes delayed if that one member was too busy to work on the project. Redundancy in the purchasing role would have handily solved this issue from the start. Our project had no team lead, which meant that no member could organize or decisively end debates. As a result, our design process was sometimes slowed by excessive argument over relatively unimportant system elements, where a commitment to a solution would have expedited the design process, allowing more time to devote to other areas of the design. In addition, this also meant that purchases would sometimes be delayed when members were unsure if there was enough agreement in the group to authorize purchases, which sometimes delayed assembly.

## B.3 Individual Contributions and Responsibilities

Every team member was regularly involved in the assembly and operation of the system throughout the duration of spring quarter, but every member also had their own unique contributions, detailed below.

Nicholas fulfilled the majority of purchases through PurchasePATH, filled out the LabRAT risk assessment form, and performed other administrative tasks in Winter quarter. He was responsible for wiring the system's pressure PID controller before this system was removed from the final design. He created some of the initial CAD models

of the system before Noah and later Chris assumed responsibility for this. He performed pressure vessel and bolt strength calculations on our provided pressure vessel to calculate its pressure rating.

Auden worked on the main design idea of using a liquid heating component during the winter quarter and explored the approval process for the secondary pressure vessel. He researched the effects of $CO_2$ saturation into water and the duration required depending on the depth of the water. He worked on construction of the assembly, including fastening pipes, valves, and other connections for the assembly device. He set up many of the initial experiments and helped reconstruct the assembly after Noah had identified broken seals on the valves.

Ella focused on researching the effects of high-pressure $CO_2$ on the saturation process in regard to saturation time as well as structure of the plastic sample. She worked on coding a model for the saturation time of the plastic sample, as well as a model for the liquid flowrate into the sample chamber. She contributed significantly to the Expo Presentation and Final Report deliverables, and helped with changing conditions for the experimentation process when initial tests were not working.

Noah worked on most of the Solidworks models during spring quarter, including designing the fluid reservoir assembly. He assisted in creating bills of materials for purchases and contributed most of the documentation of meeting notes. Along with Chris, he fabricated new PEI seals for the ball valves used in the design. Near the end of the project, he was responsible for many of the last-minute purchases.

Chris assisted with assembly of the system including fastening pipes, valves, and other parts of the system as well as cutting and assembling extrusions for the framing with Noah. He also modeled and printed brackets used to fasten some components to the frame and with Noah, machined new PEI seals when the original PTFE valve seals began to fail. Due to living on campus, he was able to assist in running many of the tests and periodically checked in on the system while it was foaming to observe for any gas leakage. He also helped organize the shipping of returns to McMaster-Carr and later made a complete CAD model of the system after the original CAD model corrupted.

# C Final project schedule or Gantt chart

The following list of milestones was created at the beginning of spring quarter and updated throughout. Some items were eventually deemed unnecessary, and others were added later as the design changed. Progress was tracked using a color-coding scheme. By June 6$^{th}$, all items had been marked either complete or no longer necessary.

- Complete system design
    - Finish sample chamber model—Apr 4
    - Determine and validate all pressure and temperature values—Apr 10
- Inquire into the chamber certification process, consulting Brian Pinkard from Aquagga, Seattle Boilerworks—Apr 7
- Internally validate sample chamber design including performing FEA (must finish before we send a design for certification)—Apr 7
- Send chamber design for certification—based on the above
- Get certification for sample chamber design—Apr 21
- Complete safety assessments and plans

    - LabRAT risk assessment tool—May 9
    - Create a standard operating procedure (SOP) for the system (included in the LabRAT)—May 9
- Order or buy all tubing, piping, connections, and sample chamber materials
    - Sample chamber stock and hardware (now the fluid reservoir)
    - Everything else (dependent on design finalized)—Apr 10 (we still need all the components listed in the meeting notes for 4-18)
- Assemble full system—May 8
- Receive all materials—May 8
- Assemble fluid chamber+heater subsystem—May 8
- Assemble depressurization and safety systems—May 8
- Assemble pressurization and pressure sensor system—May 8
- Cut and assemble all aluminum framing—May 8
- Testing
    - Inquire into SEM analysis—Apr 6
    - Heater test—May 8
    - Start first test—May 9
    - Complete first test—May 10
    - Perform SEM analysis—May 16
    - Fix valves and reassemble system—May 18
    - Run second test—May 12
    - Run third test—May 16
    - Receive SEM results—May 22
- ME 494 deliverables:
    - Critical design review—Apr 7
    - Expo project form
    - Draft report for Meza—May 12
    - Updated draft—TBD
    - Expo Poster Peer Review— May 16 or 18
    - Expo poster—May 24
    - Expo—May 30
    - Final Report—June 6

# D Pressure Validation Test

A pressure validation was performed on 11 May 2023, with the system being pressurized to roughly 3 MPa in stages. After the system was pressurized to 3 MPa all of the connections were then checked for potential leaks, and no leaks were detected at this stage. After there was determined that there were no leaks, full pressurization was done, with the system reaching roughly 5.7 MPa as expected. Again, there were no leaks detected, and at that point the system was depressurized using the ventilation hose.

# E Heater Validation Test

The heater was tested several times to learn more about the efficiency of the heating apparatus. The heater was ordered from McMaster-Carr, and is a cable heater comprised of ceramic, glass, fiberglass, and metal. If more information is desired, the item number from McMaster-Carr is 4550T133. To test the heater, the heating device was wrapped around the pipe comprising of the liquid pressure chamber and the heater was turned on to a

temperature of 100C to attempt to boil the water. No steam was observed leaving the exhaust pipe, which showed that the heater would have to be set to a higher temperature than the water. Due to the results of the validation test the engineering team also settled on a significant heating time to allow the water to equilibrate at a temperature.

# F Sample Validation Tests

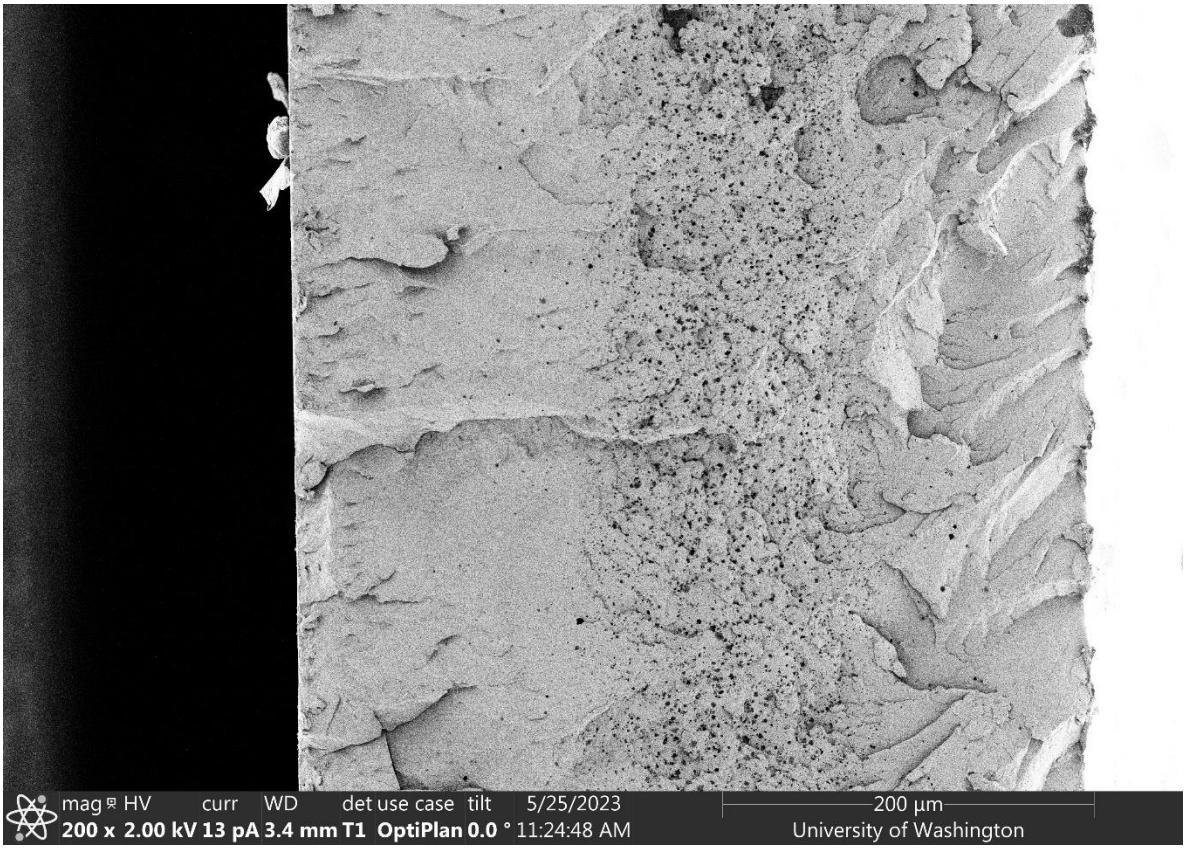


*Figure 17: Micrometer-scale SEM image showing internal structure of Sample #001, a 500-micron PET sample pressurized at 6.0 MPa and foamed at 140 C with unsaturated tap water. Image produced by Santhosh Sridhar.*

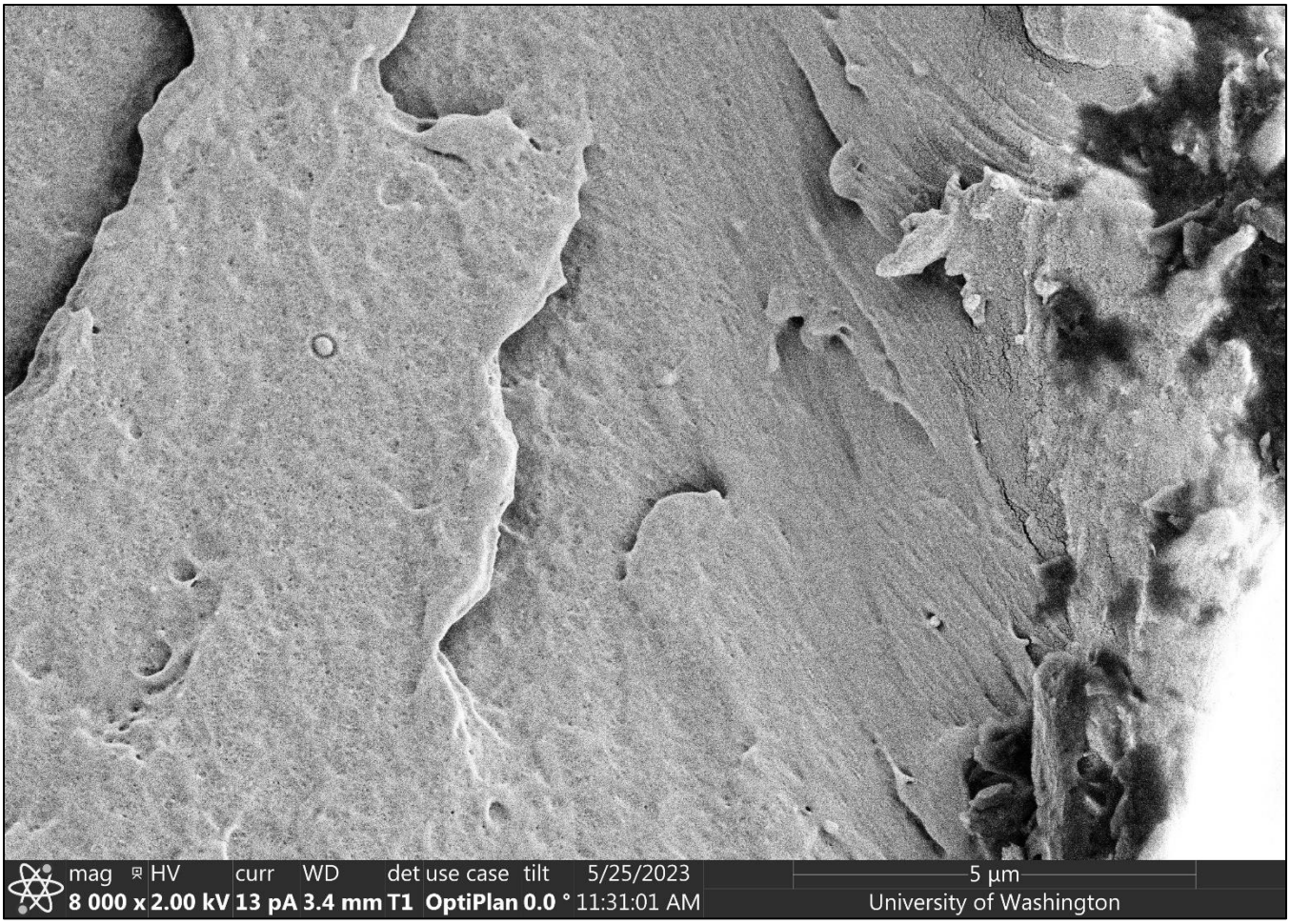


*Figure 18: Micrometer-scale SEM image showing internal surface of Sample #001, Image produced by Santhosh Sridhar.*


*Figure 19: Micrometer-scale SEM image showing internal surface of Sample #001, Image produced by Santhosh Sridhar.*

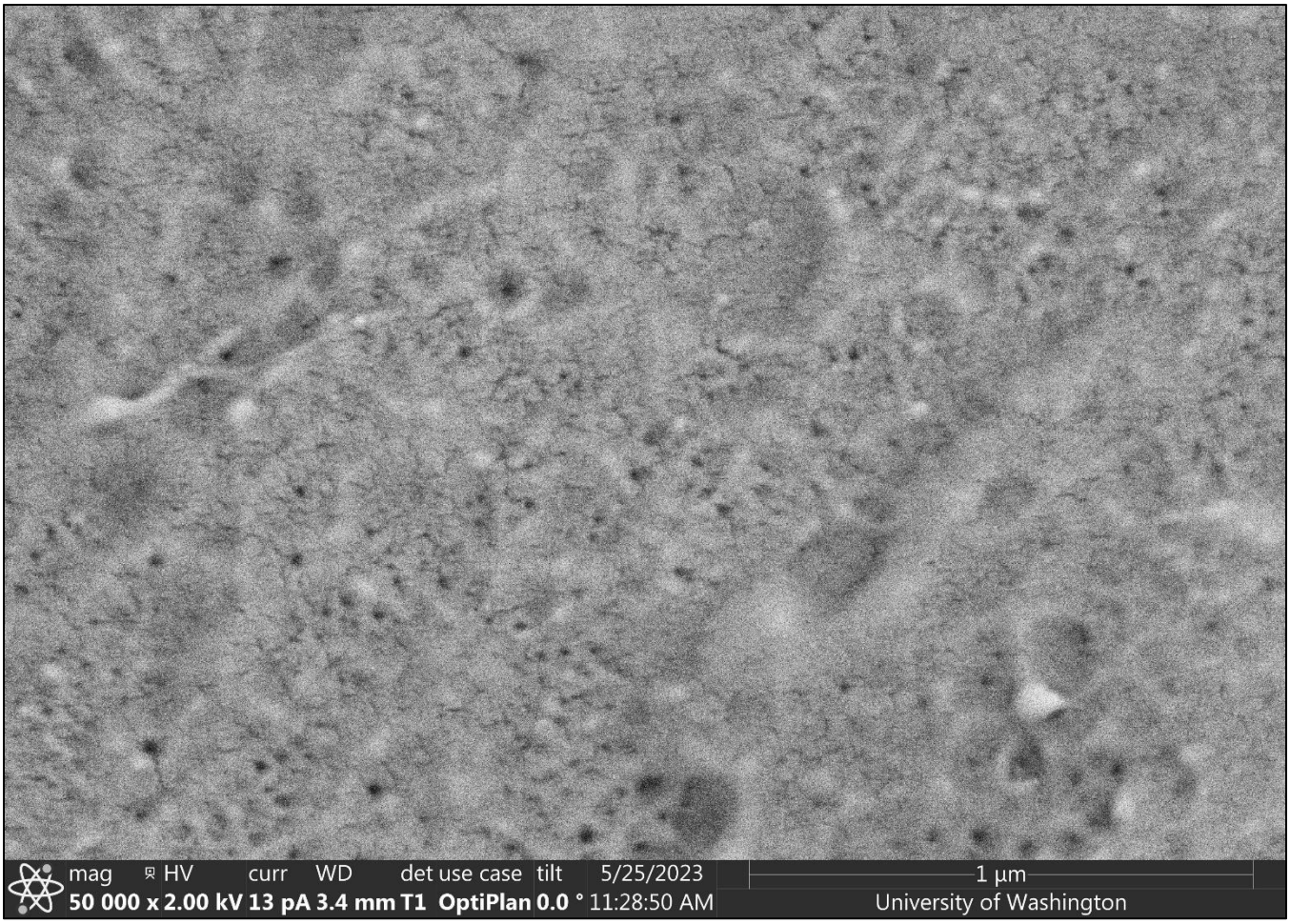


*Figure 20: Micrometer-scale SEM image showing internal surface of Sample #001, Image produced by Santhosh Sridhar.*